New developments in optoacoustics

G. A. Askar'yan and A. V. Yurkin

Institute of General Physics of the Academy of Sciences of the USSR
Usp. Fiz. Nauk **157**, 667–681 (April 1989)

A review of current research in optoacoustics. The authors describe and examine several new developments in the field: guided transport of sound in the wake of a light beam; new techniques of detecting objects in transparent and turbid media; high-resolution nonlinear subsurface imaging using self-focused beams and guided transport of the response signal; control of the spectrum and amplitude of a thermoacoustic pulse due to cropping of the light beam cross-section, lateral contact with an interface, semi-submerged light beam, and so forth. Enhancement of acoustic transmissivity by means of a laser beam is examined. The authors indicate the practical applications of these new developments.

1. INTRODUCTION

The first experimental studies of laser interaction with liquids demonstrated that the development of lasers opened a new era in the evolution of optoacoustics.[1] The new possibilities included not only the generation of powerful and even hydraulic ultra and hypersound pulses[1] by using intense or well-focused laser beams, but also the remote, contactless sound generation made possible by the high directionality of laser light.

In recent years the field of laser optoacoustics has undergone explosive growth (for reviews see Refs. 2–5). The remote generation of sound by laser beams has found wide application in hydroacoustics, led to the development of a new class of "optoacoustic" antennae, and provided new means for remote sensing, subsurface imaging, and detection.

Nonetheless, despite the profusion of optoacoustic investigations, much fundamental research remains to be done.

In this report we review our recent investigations of several new developments in optoacoustics: sound propagation in the wake of a light beam,[6] control of the spectrum and amplitude of optothermal sound,[7] light-induced changes in the viscosity and sound absorption of a medium,[8] and new techniques in nonlinear optoacoustic subsurface imaging.[9]

2. SOUND PROPAGATION IN THE WAKE OF A LIGHT BEAM

In nearly all practical applications, sound beams diverge strongly. This happens because the acoustic wavelength cannot be made arbitrarily small since sound absorption increases strongly with frequency (the classical result is $\alpha_s \sim f^2$). For example, the optimal frequencies in hydroacoustics lie in the 30–100 kHz range, i.e., the wavelength exceeds 1 cm. This corresponds to a diffractive divergence angle $\theta_D \sim \lambda_s/a > 3\cdot 10^{-2}$ rad, where a is the beam radius. An analogous situation occurs in the generation of hypersound at the focal point of a laser beam: in the case of stimulated Brillouin scattering for example, the acoustic wavelength is small, but so is the radius of the original focal spot.

The large divergence of sound waves results in a strong damping of their amplitude with distance. Can this divergence be suppressed?

One of the possibilities involves acoustic self-focusing, proposed already in 1966 by Askar'yan[10] and experimentally observed in Ref. 11 and, subsequently, in Ref. 12. Unfortunately, this method requires that the medium be subjected to intense acoustic waves for a protracted period of time, which is often impracticable.

However, Askar'yan[10] also proposed an alternative method of creating an acoustic line by employing the wake of a light beam. This phenomenon, involving a combination of nonlinear interactions, was experimentally investigated in Ref. 6.

If the light beam is to form an acoustic line, the sound velocity inside the wake must be lower than at the outside boundaries. This can be achieved in two ways: lowering the sound velocity on the beam axis or enhancing it at the boundaries. Trapping of the sound waves occurs when the condition for refraction (or total internal reflection) is reached. By analogy with optics this condition can be written as $\theta_D^2 \sim \Delta n/n \approx \Delta c_s/c_s$.

This condition is easily derived by comparing the diffraction angle θ_D, corresponding to the Fresnel length $L_F \approx a/\theta_D \sim a^2/\lambda$ (after propagating this distance diffractive beam broadening becomes significant), with the rotation angle θ_{rot} of the boundary beam due to the difference in the sound velocity on-axis and at the boundaries, $\theta_{rot} \sim (\Delta c/a)L/c$. Equating θ_{rot} with θ_D we immediately obtain the trapping condition $\theta_D^2 \sim \Delta c_s/c_s$.

The two dominant processes which can alter the sound velocity in the wake of an intense light beam (in a liquid, for example) are heating and bubble formation.

Heating changes the sound velocity by the quantity $\Delta c_s \approx (dc_s/dT)\Delta T$. For water over a wide range of temperatures $dc_s/dT \approx 4$–5 m/s deg > 0, i.e., a hollow light beam must be used. The change in temperature can be estimated as $\Delta T \approx \alpha I t/C\rho$, where α is the light absorption coefficient (cm^{-1}), I is the radiant flux density, t is the interaction time, and $C\rho$ is the heat capacity of the medium (cm^{-3}).

For instance, for the typical parameters of an unfocused laser beam produced by the neodymium laser based on a GOS-1001 device—$q \approx It \sim Q/S \approx 60$ J/cm^2, $\alpha \approx 0.15$ cm^{-1}, total energy flux $Q \approx 10^3$ J, beam cross-section $S \approx 15$ cm^2, and $C\rho \approx 4$ J/cm^3, we obtain $\Delta T \approx 2.5$ °C and $\Delta n \sim 10^{-2}$, i.e.,

 0038-5670/89/040349-08$01.80

a diffraction angle $\theta_D \approx 0.1$ rad is attained. These parameters, however, correspond to full absorption of the laser beam over approximately 6 cm. In order to extend the distance over which these phenomena can be observed, we must use radiation that is weakly absorbed ($\alpha \approx 10^{-2} \div 10^{-3}$ cm^{-1}), which reduces the changes in temperature and the corresponding nonlinear steps.

However, if the medium (i.e., water) contains a suspension of small particles, the local heating of the particle surfaces and the surrounding layers of water can be significant:

$$\Delta T_{\text{loc}} \sim \frac{It}{C\rho (\varkappa t)^{1/2}} \sim \frac{I}{C\rho}\left(\frac{t}{\varkappa}\right)^{1/2} \gg \Delta T_{\text{av}},$$

where $\varkappa$ is the thermal conductivity of the medium or the particle.

This local heating may lead to bubble formation, as gas evolves from the liquid or the suspended particles (gas solubility decreases at higher temperatures), or to particle sublimation, water evaporation, etc.

The bubbles can persist for a sufficiently long time not only because of the heating-induced supersaturation, but also because of the natural carbonation of the liquid.

Our experiments demonstrated that bubble formation can markedly affect the sound velocity in the liquid. Indeed, the sound velocity depends on the compressibility of the liquid, which can be significantly affected by the presence of bubbles. Changes in the compressibility are related to the dynamics of bubble oscillations. Each bubble is a resonant system whose intrinsic oscillation frequency depends on the mass of the displaced liquid $m \sim \rho a^3$ and the elasticity of the gas contained in the bubble

$$K = \frac{\Delta F}{\Delta a} \sim a p_0 \cdot 3\gamma$$

From the condition $pa^{3\gamma} \approx$ const. or

$$\frac{\Delta p}{p} \approx 3\gamma \frac{\Delta a}{a},$$

where Δa is the oscillation amplitude of the bubble radius a, we obtain the resonant bubble oscillation frequency

$$f_r = \frac{1}{2\pi}\left(\frac{K}{m}\right)^{1/2} \approx \frac{1}{2\pi a}\left(\frac{3\gamma p_0}{\rho}\right)^{1/2}.$$

If the sound frequency is below this resonant frequency, the bubble oscillates quasistatically. In other words, the bubble is compressed when the external pressure increases. Consequently, the compressibility of the liquid increases sharply in the presence of bubbles and the sound velocity is reduced. On the other hand, if the sound frequency is above the resonant frequency, the bubbles oscillate in antiphase: they grow as the pressure increases, thereby contributing to the rigidity of the liquid and enhancing the sound velocity.

Ignoring for simplicity the damping of bubble oscillations, the total change in sound velocity due to bubble formation is:

$$c_s^{-2} = c_{s0}^{-2} + \frac{Na}{\pi (f_r^2 - f^2)}, \quad \Delta c_s = -\frac{aNc_s^3}{2\pi (f_r^2 - f^2)},$$

where a is the mean bubble radius; N is their concentration; c_s is the speed of sound; f is the sound frequency. Which nonlinearity will dominate depends on the energy flux of the light beam and the properties of the liquid (carbonation, presence of suspended particles, and so forth).

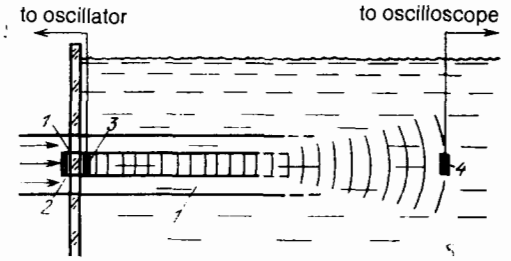

FIG. 1. Experimental apparatus for studying sound propagation in the wake of a laser beam: *1*—laser beam; *2*—washer; *3*—acoustic transducer; *4*—acoustic receiver.

We were the first to observe the guided transport of sound in the wake of a light beam,[6] as originally proposed in Ref. 10. The experiment was performed using a neodymium laser whose beam passed through a 50-liter tank of water (Fig. 1). The laser was operated either in the free-running regime (with 300 J energy) with or without telescopic beam contraction, or in the Q-switched regime with a passive solid-state shutter of LiF with F-centers serving as the beam modulator. In the latter case the beam energy was 10 J and no beam contraction was used.

The experiment involved the use of a hollow laser beam *1* (see Fig. 1). The on-axis beam intensity was reduced by a washer *2* of 0.5 cm diameter placed on top of the window in the water tank. The sound transducer *3* was located on the beam axis, as was the receiver *4* at a distance of 35 cm. The washer *2* was acoustically isolated from the tank.

In pure water, using the free-running laser beam with telescopic beam contraction, we immediately observed sound focusing in the thermal wake. The hollow beam heated the water by $\Delta T \approx Q_1/C\rho L_a \sim 10^0$ with the incident energy $Q_1 \approx Q/\pi(R_1^2 - R_2^2)$ in the contracted beam, $C\rho \approx 4$ J/cm^3, and absorption length $L_a \approx 6$ cm. This produced $\Delta c_s/c_s \approx 3 \cdot 10^{-2}$. The resulting change in the refractive index for acoustic waves Δn_s led to beam trapping for angles $\theta \sim (\Delta n_s)^{1/2} \sim 0.2$ rad. The diffractive divergence angle of the sound beam was $\theta_a \sim \lambda_s/d < 0.3$ rad, i.e., acoustic beam trapping was achieved.

Since the receiver was located at a distance several times larger than the absorption length, sound focusing did not occur over the entire propagation length L. After propagating a distance L without focusing the sound beam would have the radius $a \sim a_0 + \theta_D L$, whereas focusing over some part of the distance L_1 would produce a beam radius of $a \sim a_0 + \theta_D (L - L_1)$. Hence, given a small initial beam radius a_0, the sound amplitude should be enhanced by a factor of $L_1/(L - L_1)$. In our experiment $L \approx 35$ cm and $L_1 \approx 10$ cm; the expected acoustic amplitude enhancement by a factor of 1.5–2 was confirmed by the experimentally measured two-fold enhancement. In Fig. 2 we show the oscilloscope traces of the signal from the piezoelectric receiver. Figure 2a corresponds to the free-running laser regime with telescopic beam contraction. We show the onset of sound amplification (sweep rate is 0.5 ms/div). The duration of sound amplification ranged up to 1 s, i.e., the guiding wake forms rapidly (during the laser pulse) and persists for a very long time, until convection disperses it away from the sound beam.

We also employed a Q-switched laser to produce a bub-

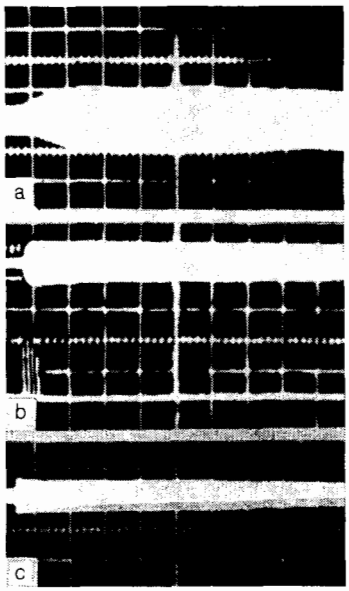

FIG. 2. Signals from the piezoelectric receiver during sound propagation in the wake of a laser beam. a—Onset of amplification (sweep rate is 0.5 ms/div). b, c—Acoustic focusing by the bubbly wake of a giant laser pulse in a medium with suspensions: b—onset of amplification (sweep rate is 1 ms/div); c—focusing of 60 kHz sound in fresh tap water (sweep rate is 25 ms/div). The sweep is triggered before the laser pulse.

bly wake. An uncontracted hollow beam passed through water which contained a small concentration of suspended particles. These particles served as nucleation centers for bubble formation during pulsed local heating of the water (the small dimensions of suspended particles ensured long settling times of ~ 3 days). The bubbles could grow at the expense of the dissolved gas. This type of acoustic line provided large discontinuities in acoustic parameters and yet required but a small energy expenditure per unit length. The oscilloscope traces of sound focusing for this process are shown in Figs. 2b and 2c: Fig. 2b shows the onset of the focusing (sweep rate is 1 ms/div), whereas Fig. 2c shows persistent focusing after 0.5 s. Note that at the operating frequency $f \sim 1$ MHz the resonant bubbles are a fraction of a micron in size, i.e., the focusing is probably due to an increase in the sound velocity in the wake ($f > f_r$). However, sound enhancement can also occur in the opposite situation, when the speed in the wake is reduced. In that case focusing occurs due to reflection at the acoustic boundary which cannot be regarded as smooth.

Since our liquid could evolve gas and hence markedly alter the sound velocity, we were able to achieve the guided transport and trapping of 60 kHz sound waves, despite their large divergence (see Fig. 2c, sweep rate is 0.25 ms/div).

When the piezoelectric transducer and receiver were interchanged we observed signal amplification because the laser beam produced an optothermal receiving acoustic line and concentrator at the receiver.

The observed phenomena can be employed to control sound propagation not only in acoustic processes, but also in hyperacoustic stimulated Brillouin scattering. By modifying the light beam profile one can focus or defocus hypersound, tune the interaction length of light and sound, and alter the nonlinear effect exerted by the hypersound on the medium.

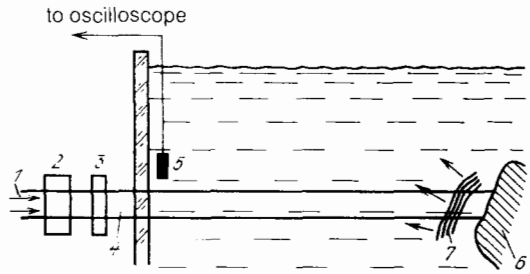

FIG. 3. Experimental apparatus for the optothermoacoustic detection of concealed objects: *1*—laser beam; *2*—KDP crystal; *3*—C3 filter; *4*—green light; *5*—receiver; *6*—concealed object; *7*—acoustic pulse.

3. OPTOTHERMOACOUSTIC DETECTION AND PROBING OF INHOMOGENEITIES IN TRANSPARENT AND TURBID MEDIA[6]

The detection of inhomogeneities in various media using reflected light may be hindered if the layer containing the inhomogeneities is turbid, or if the inhomogeneity absorbs or does not reflect light. In such a case one can turn to optoacoustics: the object is located using the sound pulse generated when light is absorbed at the surface of the object or the boundary of the absorbing layer.

We have studied experimentally this type of optoacoustic subsurface imaging. A horizontal variant of the experimental apparatus is illustrated in Fig. 3.

The pulses from a Q-switched laser *1* had an energy of 10 J (see Fig. 3). They passed through a KDP crystal *2* and a C3 filter *3*, which filtered out the fundamental frequency. The remaining green light beam *4* entered the water tank

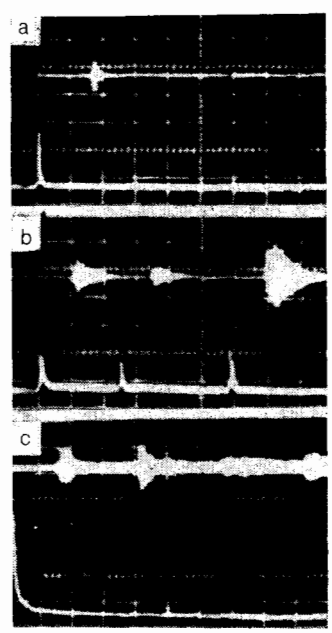

FIG. 4. Signals recorded during the optoacoustic detection of concealed objects by green laser light. Lower traces: laser pulses; upper traces: signals from the piezoelectric receiver. a—Detection of a blackened metal cylinder in water using giant laser pulses (sweep rate is 100 μs/div). b—Signals from a rubber coating (sweep rate is 50 μs/div). c—Signals from a vertical laser beam incident on a bottom layer of silt: the first pulse is the thermoacoustic signal generated by absorption of light at the surface; the second pulse is the thermoacoustic signal transmitted into the layer and reflected from the bottom ($h_1 = 10$ cm, $h_2 = 19$ cm, sweep rate is 50 μs/div).

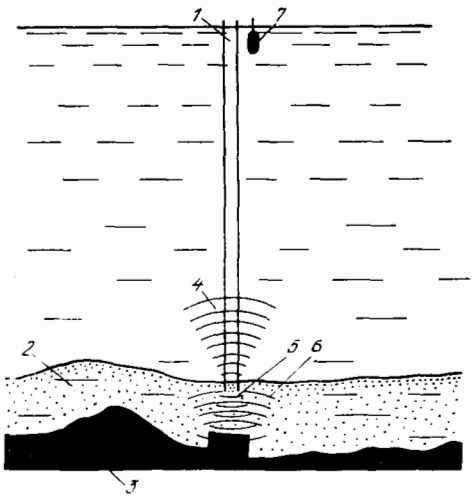

FIG. 5. Detection of inhomogeneities in a bottom layer of silt. *1*—laser beam; *2*—bottom layer of silt (optical absorption interface); *3*—bottom; *4*—thermoacoustic pulse propagating upward from the absorption interface; *5*—pulse propagating downward; *6*—pulse reflected from the bottom or the inhomogeneity; *7*—receiver.

which contained a dark metallic or dielectric object and a piezoelectric receiver *5*. The time delay of the sound pulse *7* determined the distance between the receiver and the object. The mechanism giving rise to the sound pulse could arise from thermal expansion, gasification or boiling of water near the surface of the object.

In Fig. 4 we show oscilloscope traces of the laser pulses (lower traces) and piezoelectric receiver signals (upper traces): Fig. 4a contains the signal generated by a blackened metal cylinder of 10 cm diameter located 30 cm away from the receiver (sweep rate is 50 μs/div). The signal is anomalously strong, which may be explained by high absorption, low thermal conductivity, surface roughness or gasification of the surface during heating.

We also observed signals from inhomogeneities in the bulk or on the surface of plexiglass.

Optothermoacoustic subsurface imaging can be achieved even if the object is located inside an opaque medium (for example, concealed in a layer of silt at the bottom of a body of water, etc.). There the absorbed light pulse will generate thermoacoustic pulses which will generate thermoacoustic pulses which will propagate in both directions away from the absorption boundary and into the bulk of the medium (see Fig. 5). The upward-propagating pulse will arrive after a delay $t_1 = h_1/c_s$, where h_1 is the depth of the absorption boundary. The downward-propagating pulse will be reflected by the bottom or by the concealed object, and will arrive at the receiver after a delay $t_2 = [h_1 + 2(h_2 - h_1)]/c_s = (2h_2 - h_1)/c_s$, where h_2 is the total distance to the bottom or to the concealed object. The quantity h_2 can be obtained directly from the delays t_1 and t_2, $h_1 = (t_1 + t_2)/2c_s$, for arbitrary h_1.

In our experiments the green laser beam was incident on the surface of a water-filled tank. A 9 cm layer near the bottom of the tank was made turbid by the addition of an optically absorbing sol. The absorption boundary was $h_1 \approx 10$ cm deep. The upward-propagating thermoacoustic pulse generated at the boundary gave rise to the first signal (Fig. 5), while the downward-propagating pulse traversed the turbid layer, reflected from the bottom, and gave rise to the second signal. The measured quantity h_2 was quite close to the total depth (see Fig. 4c). The same technique could be employed to locate objects concealed in the turbid layer.

These studies could prove of use in thermoacoustic subsurface imaging; location of inhomogeneities in liquid, solid, and gaseous media; homogeneity monitoring; and the development of optoacoustic microscopes or optoacoustic holography systems.

The use of a probe pulse sufficiently powerful to create an acoustic line presents an intriguing possibility of reducing the divergence of acoustic signals as they propagate back towards the surface.

In this section we have discussed only one variant of nonlinear subsurface imaging. Now we shall turn to other developments in this field.

4. HIGH-RESOLUTION NONLINEAR SUBSURFACE IMAGING—NEW APPLICATIONS OF OPTICAL SELF-FOCUSING AND OPTICAL SOUND FOCUSING[9]

In the detection, observation, and probing of objects using light beams, the usual techniques rely on the optical or acoustic response generated when the beam impacts on the object. This response makes it possible to determine the distance to the object (from the time delay of the signal), its location (by scanning the beam spot), its dimensions and velocity (from its traversal of the beam spot), and its structure (from the recorded image).

In this report we examine the promise of self-focusing (for a review see Ref. 13) for improving the resolution and effectiveness of subsurface imaging.

Self-focusing is known to contract the light beam and increase its intensity, thereby enhancing the optical or acoustic response of the object. Beam contraction also improves the resolution with which an object's position can be determined. Another important feature of self-focusing is its ability to improve significantly the transport and directionality of the reflected signal.

The point is that a self-focused light beam can modify the properties of the medium and these modified properties may persist on a sufficiently long time scale to assist in the transport of the return signal.

An acoustic line based on a Kerr nonlinearity can be created rapidly (optimally in $< 10^{-11}$ s) and will exist over the duration of a Q-switched pulse ($\approx 3 \cdot 10^{-8}$ s) on a length scale $L \approx 10^3$ cm. For a striction nonlinearity, the time required to create an acoustic line, as well as its lifetime, is determined by the so-called acoustic time $t_s > a/c_s \approx 10^{-6}$ s for a beam radius $a > 0.1$ cm and sound velocity $c_s \approx 10^5$ cm/s, i.e., over distances $L \approx 3 \cdot 10^4$ cm for optical signals. In the case of thermal self-focusing, the acoustic line can persist for a very long time because of slow heat dissipation.

Irrespective of the duration of existence of the acoustic line, which ensures guided propagation of the response signal, the response signal strength is always improved by beam contraction and the accompanying intensity enhancement. The contraction rate for a fast nonlinearity can be estimated from the aberration-free nonlinear refraction equation: $a''_{zz} \approx A/a^3$, where $A \approx [(\lambda^2/2\pi) - n_2 E_0^2 a_0^2]$. Integrating twice we obtain $a(z) \approx a_0[1 - (z^2/L_f^2)]$, where $L_f \approx a_0/A^{1/2}$. The intensity enhancement $I(z) \approx P/\pi a^2(z)$ can be significant, sufficient not only for a linear increase in

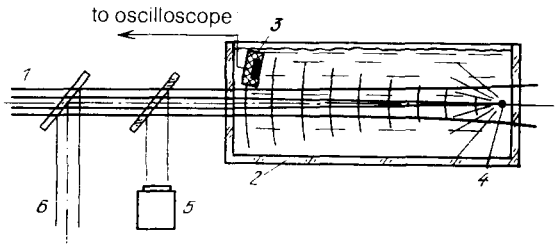

FIG. 6. Experimental apparatus for nonlinear, high-resolution subsurface imaging. *1*—Hollow laser beam; *2*—water cell; *3*—piezoelectric detector or photodetector; *4*—metal ball; *5*—FK photocell, photomultiplier tube or camera; *6*—coloring light beam from a gas laser.

the response, but also for nonlinear effects, such as increased thermoacoustic generation efficiency at the surface of the object.

We have carried out an experimental study focused on enhancing the response and improving the efficiency of subsurface imaging. For low power beams in liquids, thermal refraction is significant, leading to self-focusing of beams with reduced on-axis intensity (the so-called "banana self-focusing" of hollow beams[14]). In this case the focal length $L_f \approx d/2\theta_{nl}$, with $\theta_{nl} \sim (n'_T \Delta T)^{1/2} \approx (n'_T \alpha I t)^{1/2}/C\rho$, where n'_T is the derivative of the refractive index with respect to temperature; ΔT is the heating-induced temperature change; α is the absorption coefficient; It is the energy density of the beam; $C\rho$ is the bulk heat capacity; d is the diameter of the inner spot.

The experimental apparatus is shown in Fig. 6. The hollow laser beam *1* was produced by passing an ordinary beam through a glass plate with a small on-axis screen. This beam entered a liquid-containing cell that was 10 to 25 cm long *2*, the liquid being water or alcohol. The object to be located—a ball of 1 mm diameter—was placed near the beam axis at a distance close to the focal length. The acoustic and optical signals were recorded by an acoustic or optical receiver *3*, and a photodetector or camera *5*.

In this experiment we used a neodymium laser, whose light is strongly absorbed by water ($\alpha \approx 0.15$ cm^{-1}), so the optical signal generated by the absorption or scattering from the object was detected either at the fundamental or the second harmonic frequency (using an IR-sensitive detector, either an FK photocell or a photomultiplier tube), or by employing a coloring light *6*, for example the cw radiation of a He–Ne laser at several mW power coupled in by reflection from an angled mirror. In the case of the object located at a distance much greater than the absorption length for the main heating beam, this arrangement produced a nonlinear lens near the entry point into the liquid or near the liquid surface (at incidence from above). This lens not only focused the coloring light, but also flattened out the scattered light into a parallel beam, facilitating remote reception.

Two types of lasers were employed in the experiment.

1. The first was a neodymium laser based on a tunable, pulsed solid-state laser with a gadolinium—scandium—gallium garnet (GSGG) crystal, with a 25 Hz repetition frequency. In the modulated regime this system produced trains of 20 peaks with 20 μs intervals between the peaks. The average total power was 2–3 W. The outside beam diameter at the entry point into the water was 5 mm. The diameter of the intensity dip was 2.5 mm. This laser provided the means of rapidly acquiring the response for various positions of the object, but the duration of the trains was limited by the characteristic convection time of ~ 1 s.

2. The second laser was a neodymium laser based on a GOS-1001 device, with the same small beam diameter of 5 mm. Upon fourfold traversal of the active medium this laser produced up to 50 peaks of 0.1 J energy in a period of 1.5 ms, with 30 μs intervals between the peaks and an average total energy of 5 J. In this system the convective distortion during the laser pulse was negligible and the time between the pulses was large (8 min).

4.1. Amplification of the optical response

We observed an amplification of the optical signal—the scattered He-Ne laser light from a metallic ball—due to self-focusing of the main laser beam from the type 2 laser. Figure 7a shows the image of the object without self-focusing (either with the heating beam turned off or without on-axis intensity reduction), whereas Fig. 7b shows a bright image with a self-focused main beam. The photographs were taken on KN-4 film 1 s after the laser flash, with an exposure time of 1/30 s. The camera *5* (see Fig. 6) was aimed at the object. An analogous, albeit weaker amplification was observed with the camera pointed at an angle to the incident axis.

Figures 7c and 7d show the amplification due to self-focusing of a cross painted on the object. The image was recorded directly onto the film in the camera *5* with the ob-

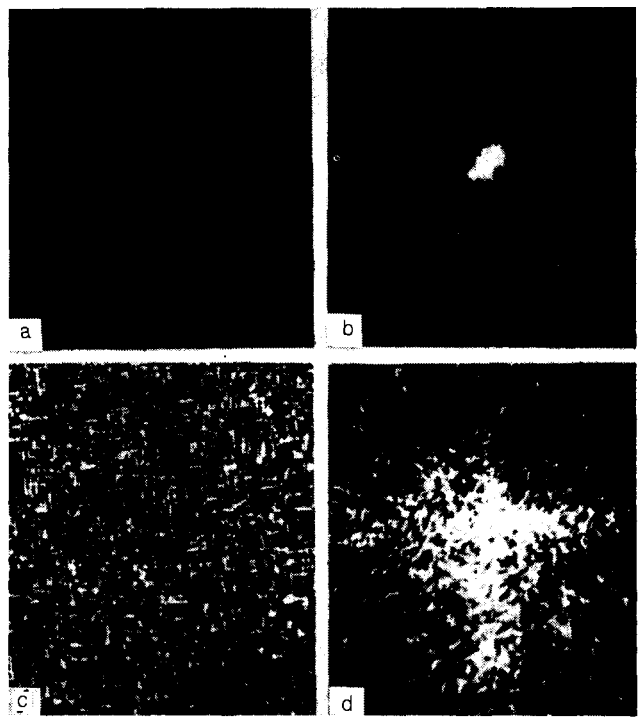

FIG. 7. Amplification of the optical response due to self-focusing. The image is recorded in the light of a He-Ne laser beam used to color the wake of the invisible main beam. a—Barely visible image of a ball (the main beam is either switched off or smoothed to eliminate self-focusing); b—hollow main beam: self-focusing occurs and the image is markedly brighter. The photographs were taken by a camera aimed at the object. c, d—Images of a cross painted on the object: structure becomes discernible due to self-focusing. Photographed directly onto film without an objective lens 1 s after the laser flash (KN-4 film, 1/30 s exposure). The main beam is from a laser based on a GOS-1001 device (type 2 in the text).

jective lens removed. This was the first image transmitted by the self-focusing mechanism.

We also investigated the amplification of the optical response over time using an FK photocell and a photomultiplier. These detectors registered the amplification of the response at the fundamental frequency. We observed a several-fold amplification of the reflection by the time a bright spot appeared on the object. In the absence of the object no nonlinear scattering was observed.

4.2. Amplification of the acoustic response

We used a piezoelectric detector to register the amplification of the thermo-acoustic response from a blackened ball due to main beam self-focusing. Using the type 1 laser we studied the distribution of the acoustic signal for various positions of the object with respect to the beam axis at different times corresponding to different stages in the nonlinear response. Figure 8 shows the distribution of the acoustic response. Curve *1* corresponds to the time by which the thermal self-focusing had developed. Curve *2* corresponds to an early time when the beam traversing the medium was still hollow. Curve *3* also corresponds to an early time, but without the intensity reduction on axis (i.e., solid beam). Finally, curve *4* corresponds to the time by which the solid beam has been thermally defocused. Clearly, given the same beam amplitude, self-focusing not only enhances the amplitude of the acoustic signal, but also improves the imaging resolution until it is limited by the size of the receiver (indicating that the resolution can be improved still further). Moreover, the position of the focal point obtained from the peak response could be compared with the distance obtained from the time delay of the incoming signal.

Let us estimate the energy expenditures required for nonlinear subsurface imaging. For simplicity we shall assume that the beam dimensions remain constant throughout the process.

In the case of a striction nonlinearity, the necessary power is $P_{cr} \approx \lambda^2 \pi^2 c/n_2$ (from the condition $\theta_D^2 \sim (\lambda/2a_0)^2 \approx n_2 E_0^2$). This power must be maintained over at least the acoustic time $t_s < a_0/c_s$ required for beam contraction, hence the energy $\mathscr{E}_{cr} \approx P_{cr} t_s \approx \lambda^2 \pi^2 ca/n_2 c_s$. A striction nonlinearity has $n_2 \approx (\partial n/\partial \rho)^2 \ (1/c_s^2) \ (\rho/2\pi) \approx 10^{-12}$ (abs. CGS units) and for the media of interest we have $P_{cr} \sim$ MW and $\mathscr{E}_{cr} \approx 10$ J.

A Kerr nonlinearity has $n_2 \approx 10^{-11}$ abs. units for the orientational Kerr effect and $n_2 \approx 10^{-14}$ for the electronic Kerr effect, but the times may be much shorter and hence the required energy may be small ($t/n_{2,\text{Kerr}} \ll t_s/n_{2,\text{strict}}$).

For intermediate power levels and thermal banana self-focusing $\theta^2 \sim \Delta n \approx n_T' q_1/C\rho$, where q_1 is the energy expenditure per unit length. Consequently the total energy is $Q \approx q_1 L \approx \pi a^2 \theta^2 C\rho L/n_T' \approx 4 \cdot 10^{-2}$ J given $\theta \approx 10^{-4}$ rad, $C\rho \approx 4$ J/cm^3·deg, $n_T' \approx 10^{-4}$ deg^{-1}, $L \approx 1$ m, and $\pi a^2 \sim$ cm^2.

For low-energy lasers these nonlinear processes are of interest not only in media with a giant nonlinearity[15] but also in ordinary media.[16]

The energy expenditures could be reduced if multiple low-power beams are focused by the thermal wake of a single, sufficiently powerful beam. This approach could prove particularly effective in media characterized by low convection, where density changes little with temperature ($\partial\rho/\partial T \to 0$). Examples include fresh water near 4 °C or salt water near 0 °C, highly viscous liquids, liquids in zero gravity, solids, and so forth, i.e., all materials where thermal dissipation of the wake is slow. Reduced energy expenditures would facilitate high resolution nonlinear subsurface imaging.

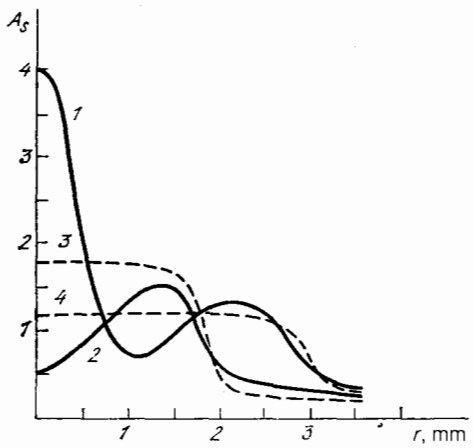

FIG. 8. Acoustic response as a function of radial distance of the object from the axis for various beams and nonlinearity stages. *1*—Signals after the formation of self-focusing (time scale of 1 s); *2*—before the formation of nonlinearity (short times); *3*—signals in the spot of an initially uniform (uncropped) beam before nonlinear effects; *4*—in the spot of a self-defocused, initially uniform (uncropped) beam. The response was measured in a train of pulses from a type 1 laser based on a GSGG crystal before the onset of convection ($t < 1$ s). Self-focusing clearly enhances the signal amplitude and improves the resolution.

5. CONTROL OF THE SPECTRUM AND AMPLITUDE OF OPTOTHERMAL SOUND BY TUNING THE LIGHT BEAM CROSS-SECTION OR BY LATERAL CONTACT WITH AN INTERFACE[7]

In recent years optothermal acoustics has developed into a separate branch of acoustics, becoming the subject of several reviews[2–4] and a monograph.[5] Nonetheless, the problem of controlling the spectrum and amplitude of an acoustic pulse still remains to be investigated in sufficient detail.

Furthermore, this problem is of considerable practical interest, as it may lead to significant progress in the reception of acoustic waves.

Usually a light beam has a smooth radial intensity distribution, especially far from the source, where diffraction and scattering smear the radial distribution of the beam. On the other hand, at short distances, before the radial distribution is smeared by diffraction, it can be used to shape an acoustic pulse, especially in the acoustic near field. If the energy is supplied over a short period, the characteristic time scale of a thermoacoustic pulse is $t_s \sim a/c_s$, where a is the beam radius. It turns out that a laser beam with sharp boundaries can be used to obtain shorter acoustic pulses of larger amplitude.

The experimental arrangement is shown in Fig. 9a. A neodymium laser beam *1* generated a giant pulse of 5 J energy and 30 ns duration. In order to equalize and smooth the edges of the intensity distribution the beam was transmitted through a matte plate *2* positioned 8 cm away from the glass window *4* of the water tank *5*. At this distance the matte plate reduced the on-axis intensity by a factor of five and broadened the sharp intensity edges into transition regions of width $\delta \approx 1.5$ cm. The average beam broadening angle was

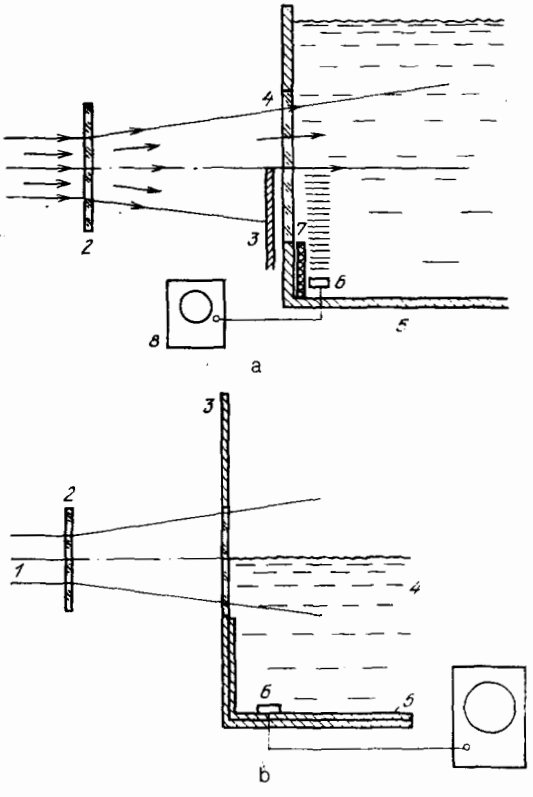

FIG. 9. Experimental arrangement for controlling the thermoacoustic pulse by selecting the type of beam cropping. a—Radial beam cropping with knife edges of various shapes: leftmost →—laser beam; *2*—matte plate; *3*—knife edge; *4*—window; *5*—liquid tank; *6*—piezoelectric transducer; *7*—sound-insulating spacer; *8*—oscilloscope. b—Semi-submerged beam: *1*—laser beam; *2*—matte plate; *3*—tank; *4*—water level; *5*—sound-insulating spacer; *6*—piezoelectric transducer.

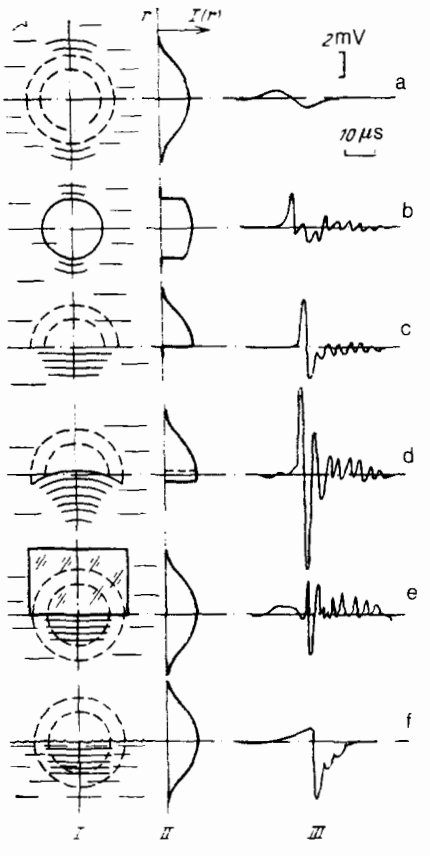

FIG. 10. Beam cross-sections (*I*) intensity distributions $I(r)$ (*II*), and oscilloscope traces of the thermoacoustic pulses (*III*) for: a—smooth distribution; b—circularly cropped beam; c—beam cropped with a straight knife edge; d—beam cropped with a curved knife edge; e—beam in lateral contact with an interface; f—semi-submerged beam.

0.2 rad. The beam cross-section was cropped by a straight or curved knife edge *3*, or a ring positioned in front of the window, or a transparent insert (glass block) immersed in the water (Fig. 10) screening a part of the light beam, or a free interface.

A nonresonant piezoelectric receiver *6* of 0.2 V/atm sensitivity was placed 6 cm above the beam axis. The receiver was mounted on an acoustically matched brass rod and the output was sent to a storage oscilloscope *8*. The piezoelectric transducer was shielded from the tank wall by a sound-insulating spacer *7* and screened from scattered light by metallized thermoplastic resin (Lavsan) foil.

The results are combined in Fig. 10: the beam cross-sections are shown in column I; the corresponding radial intensity distributions in column II; and oscilloscope traces of the resulting optothermal acoustic pulses in column III. Figure 10a corresponds to a beam with a smooth, nearly Gaussian intensity distribution, which generates a low-amplitude acoutic pulse with a smooth wavefront. Figure 10b corresponds to a circularly cropped beam (the beam is transmitted through a hole of a smaller radius). The resulting pulse is compressed by a factor of two or three and the amplitude is enhanced by the same factor. Figure 10c corresponds to a beam cropped with a straight knife edge from below with respect to the receiver: the pulse is amplified by a factor of four or five and becomes sharper still. Figure 10d features cropping with a curved knife edge, which makes it possible to focus the sound at the receiver: a ten-fold enhancement of the signal was achieved. Finally, Fig. 10e corresponds to a smoothly varying beam propagating along a sharp interface with another material characterized by different thermoacoustic or acoustic properties.

The latter case is of particular practical interest because the sound-generating light beam usually has a smooth intensity distribution at large distances from the light source. The presence of a sharp interface between different materials, for example the water surface for a partially submerged beam (see Fig. 9b), can sharply enhance the amplitude and effective frequency of the thermoacoustic pulse. We examined this situation in great detail (see Fig. 10f). In all cases the receiver was located below the beam.

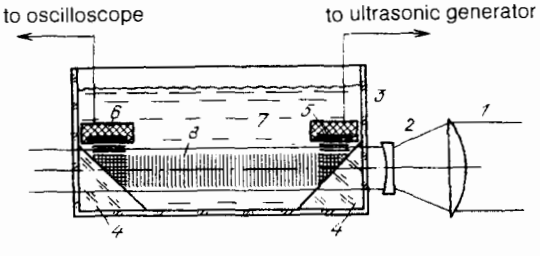

FIG. 11. Experimental apparatus for studying laser-induced transmissivity enhancement: *1*—laser beam; *2*—telescope; *3*—liquid cell; *4*—prisms; *5*—acoustic radiator; *6*—ultrasonic receiver; *7*—glycerin; *8*—laser and ultrasonic beams.

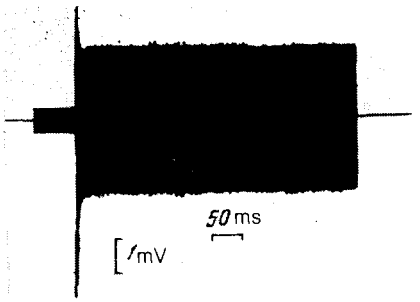

FIG. 12. Enhancement of acoustic transmissivity of the medium in the beam of a free-running laser. Retouched oscilloscope trace of the detector signal.

Analogous effects should be observable in acoustic signals produced by beams of charged particles, either injected from the outside or generated inside the medium by penetrating radiation, such as gamma rays, muons, neutrinos, etc.[4,17-23]

The observed amplitude enhancement and compression of acoustic pulses can be explained by an increase in the sharpness of the edge effects of the medium discontinuity at the boundary of the ray of diminished sound divergence (in the case of straight edge cropping) or by sound convergence (in the case of circular cropping). More detailed explanations are discussed in Ref. 7.

In addition to hydroacoustics, the foregoing results could prove useful in photoacoustic analysis: if the measured absorption coefficients of the analyzed media are small, the amplitude of the optothermal acoustic signals can be smaller still, difficult to register and even more difficult to measure. The possibility of enhancing the acoustic amplitude near the receiver could profitably extend the range of measurable absorption coefficients.

6. LASER-PULSE INDUCED CHANGES IN THE VISCOSITY AND ACOUSTIC ABSORPTION OF A MEDIUM[8]

Another recently discovered effect is the enhancement of the acoustic transparency of a medium due to optical interaction.

The experimental arrangement was quite basic. Two glass prisms were immersed in a liquid characterized by high acoustic absorption (refrigerated glycerin). The prisms and the liquid had similar indices of refraction. A rapidly pulsed laser beam propagated almost rectilinearly through the prisms, heating the liquid and reducing its acoustic absorption. The first prism reflected the acoustic signal in the direction of the laser beam, while the second prism redirected the signal to the receiver (Fig. 11).

In Fig. 12 we show the signal from the receiver, indicating a six-fold enhancement of acoustic transmissivity.

Such systems can be used as acoustic shutters (compare with the inhibition of sound transmission by a vapor film formed on the interface due to laser irradiation or pulsed electrolysis[24-26]). Light-induced acoustic transmissivity enhancement can be much faster and more efficient than thermal self-effects in powerful acoustic beams.[11,27]

This effect could be particularly pronounced at higher frequencies (usually sound absorption $\alpha \sim f^2$) over distances L for which the product $\alpha(f)L$ can be altered significantly by optical heating.

7. CONCLUSION

The research described in this report reflects the varied and inexhaustible nature of the optoacoustic interaction.

[1)]Translator's note. Presumably the Russian acronym VRMB stands for "stimulated scattering of Mandel'shtam-Brillouin".

[1]G. A. Askar'yan, A. M. Prokhorov, G. F. Chanturiya, and G. P. Shipulo, Zh. Eskp. Teor. Fiz. **44**, 2180 (1963) [Sov. Phys. JETP **17**, 1463 (1963)].
[2]F. V. Bunkin and V. M. Komissarov, Akust. Zh. **19**, 305 (1973) [Sov. Phys. Acoust. **19**, 203 (1973)].
[3]L. M. Lyamshev, Usp. Fiz. Nauk **135**, 637 (1981) [Sov. Phys. Usp. **24**, 977 (1981)].
[4]L. M. Lyamshev (ed.), Radiation Acoustics: Collected Articles [in Russian], Nauka, M., 1987.
[5]B. K. Novikov, O. V. Rudenko, and V. I. Timoshenko, Nonlinear Hydroacoustics, Acoust. Soc. Amer., N.Y., 1987 [Russ. original, Sudostroenie, Leningrad, 1981].
[6]G. A. Askar'yan and A. V. Yurkin, Pis'ma Zh. Eskp. Teor. Fiz. **43**, 175 (1986) [JETP Lett. **43**, 221 (1986)].
[7]G. A. Askar'yan and A. V. Yurkin, Akust. Zh. **33**, 370 (1987) [Sov. Phys. Acoust. **33**, 219 (1987)].
[8]G. A. Askar'yan and A. V. Yurkin, Akust. Zh. **33**, 1121 (1987) [Sov. Phys. Acoust. **33**, 655 (1987)].
[9]G. A. Askar'yan and A. V. Yurkin, Pis'ma Zh. Eksp. Teor. Fiz. **47**, 494 (1988) [JETP Lett. **47**, 579 (1988)].
[10]G. A. Askar'yan, Pis'ma Zh. Eksp. Teor. Fiz. **4**, 144 (1966) [JETP Lett. **4**, 99 (1966)].
[11]V. A. Assman, F. V. Bunkin, A. V. Vernik, G. A. Lyakhov, and K. F. Shipilov, Pis'ma Zh. Eksp. Teor. Fiz. **41**, 148 (1985) [JETP Lett. **41**, 182 (1985)].
[12]V. G. Andreev, A. A. Karabutov, O. V. Rudenko, and O. A. Sapozhnikov, Pis'ma Zh. Eksp. Teor. Fiz. **41**, 381 (1985) [JETP Lett. **41**, 466 (1985)].
[13]G. A. Askar'yan, Usp. Fiz. Nauk **107**, 507 (1972) [Sov. Phys. Usp. **15**, 517 (1972-73)]; Usp. Fiz. Nauk **111**, 249 (1973) [Sov. Phys. Usp. **16**, 680 (1973-74)].
[14]G. A. Askar'yan and V. B. Studenov, Pis'ma Zh. Eskp. Teor. Fiz. **10**, 113 (1969)].
[15]B. Ya. Zel'dovich, A. V. Sukhov, and N. F. Pilipetskiĭ, Kvant. Élektron. **10**, 1022 (1983) [Sov. J. Quantum Electron. **13**, 645 (1983)].
[16]G. A. Askar'yan, A. A. Lerman, and M. A. Mukhamedzhanov, Kvant. Élektron. **14**, 2045 (1987) [Sov. J. Quantum Electron. **17**, 1305 (1987)].
[17]G. A. Askar'yan, G. P. Mkheidze, and A. A. Savin, Pis'ma Zh. Tekh. Fiz. **10**, 1465 (1984) [Sov. Tech. Phys. Lett. **10**, 619 (1984)].
[18]G. A. Askar'yan and N. M. Tarasov, Pis'ma Zh. Eksp. Teor. Fiz. **20**, 277 (1974) [JETP Lett. **20**, 123 (1974)].
[19]G. A. Askar'yan, At. Énerg. **3**, 152 (1957).
[20]G. A. Askar'yan and B. A. Dolgoshein, Pis'ma Zh. Eksp. Teor. Fiz. **25**, 232 (1977) [JETP Lett. **25**, 213 (1977)].
[21]G. A. Askar'jan (Askar'yan), B. A. Dolgoshein, A. N. Kalinovsky (Kalinovskiĭ), and A. V. Mokhov, Nucl. Instrum. Meth. **164**, 267 (1979).
[22]A. de Rujula, S. L. Glashow, R. Wilson, and G. Charpak, Phys. Rep. **99**, 341 (1983).
[23]G. A. Askar'yan, Usp. Fiz. Nauk **144**, 523 (1984) [Sov. Phys. Usp. **27**, 846 (1984)].
[24]G. A. Askar'yan and T. G. Rakhmanina, Zh. Eskp. Teor. Fiz. **61**, 1199 (1971) [Sov. Phys. JETP **34**, 639 (1972)].
[25]G. A. Askar'yan, É. Ya. Gol'ts, and T. G. Rakhmanina, Zh. Eksp. Teor. Fiz. **62**, 1072 (1972) [Sov. Phys. JETP **34**, 639 (1972)].
[26]G. A. Askar'yan, E. F. Bol'shakov, É. Ya. Gol'ts, and V. P. Logvinenko, Zh. Eksp. Teor. Fiz. **64**, 1154 (1973) [Sov. Phys. JETP **37**, 587 (1973)].
[27]V. A. Assman and K. F. Shipilov, Akust. Zh. **32**, 754 (1986) [Sov. Phys. Acoust. **32**, 472 (1986)].

Translated by A. Zaslavsky